be smaller than those at the bottom of conduction band. For type B and C samples, nonparabolicity of the conduction band will be more severe, because of the higher value of Φ_0.

Another factor which should have caused a discrepancy from the simple thermionic emission equation is the effect of scattering. Although the scattering mechanisms are complex, as a crude approximation, we assume that only a portion of electrons within a narrow directional cone as shown in Fig. 1(b) can reach the intrinsic gate without collision, otherwise they will experience scattering and will not contribute to the thermionic emission current. Then the maximum ballistic solid angle can be expressed by $2\pi\theta_M = 2\pi\cos^{-1}(W_{\rm gs}/L_{\rm av})$, where $L_{\rm av}$ is the mean free path of electrons. Because the mean free path will be much smaller with increasing electron energy due to excitation of optical phonons, the above equation can not be applicable in real situations. However, at least it can be said that the effect of the scattering will be severe when $W_{\rm gs}$ becomes close to some critical value corresponding to the mean free path. In our PDB diode structure, $W_{\rm gs}$ for type A and B samples is the same and is almost three times larger than that for type C sample, and the potential barrier height Φ_0 for type A sample is the lowest among these three samples. So that the differences in the experimentally determined values γ_F for three type samples, 7.4% (A), 0.3% (B), 0.8% (C), can be explained qualitatively. For more quantitative discussion of the ballistic transport factor, diode structures with further lower potential barriers will be necessary to eliminate the complexity of the GaAs band structure.

IV. Conclusion

The I–V characteristics of GaAs PDB diode structures grown by MLE with electrically measured source-drain distances from 500 Å to 950 Å have been measured at temperatures ranging from 77 K to 423 K. The carrier injection by static induction mechanism was confirmed experimentally. The small values of γ_F were explained qualitatively by the nonparabolicity of the band structure and scattering which confines the ballistic electrons within the maximum ballistic solid angle. It means that to get larger γ_F, the barrier height Φ_0 should be designed lower. At low temperature, the current probably due to tunneling requires further study.

Acknowledgment

The authors would like to thank Dr. Kurabayashi, and Mr. Kikuchi and Mr. Henmi for the fabrication of MLE sample wafers.

References

[1] J. Nishizawa, T. Terasaki, and J. Shibata, "Field-effect transistor versus analog transistor (static induction transistor)," *IEEE Trans. Electron Devices*, vol. ED-22, pp. 185–197, 1975.

[2] J. Nishizawa and K. Motoya, "SIT as ballistic device," *Topics in Millimeter Wave Technology*, K. J. Button, Ed. New York: Academic, 1988, vol. 2, pp. 213–247.

[3] J. Nishizawa, H. Abe, and T. Kurabayashi, "Molecular layer epitaxy," *J. Electrochem. Soc.*, vol. 132, pp. 1197–1200, 1985.

[4] R. J. Malik, T. R. Aucoin, R. T. Ross, K. Board, C. E. C. Wood, and L. F. Eastman, "Planar-doped barriers in GaAs by molecular beam epitaxy," *Electron. Lett.*, vol. 16, pp. 836–837, 1980.

[5] R. F. Kazarinov and S. Luryi, "Charge injection over triangular barriers in unipolar semiconductor structures," *Appl. Phys. Lett.*, vol. 38, no. 10, pp. 810–812, 1981.

[6] A. C. Gossard, R. F. Kazarinov, S. Luryi, and W. Wiegmann, "Electric properties of unipolar GaAs structures with ultrathin triangular barriers," *Appl. Phys. Lett.*, vol. 40, no. 9, pp. 832–833, 1982.

[7] P. Plotka, T. Kurabayashi, Y. Oyama, and J. Nishizawa, "Ideal static induction transistor implemented with molecular layer epitaxy," *Appl. Surf. Sci.*, vol. 82/83, pp. 91–96, 1994.

[8] Y. Oyama, P. Plotka, and J. Nishizawa, "Selective MLE growth of GaAs and surface treatment for ideal static induction transistor (ISIT) application," *Appl. Surf. Sci.*, vol. 82/83, pp. 41–45, 1994.

Dependence of the Injection Current at Lasing Threshold on Structure and Losses in AlGaN/GaN Lasers

Pankaj Shah and Vladimir Mitin

***Abstract*—We present calculations of the threshold current densities, $J_{\rm th}$, in AlGaN/GaN double heterostructure lasers for different active region thickness, losses, and cavity lengths. Two-dimensional (2-D) numerical simulations indicate that for a 100-μm long cavity, a 0.1-μm thick active region gives the lowest $J_{\rm th}$ when only mirror losses are present. As losses increase, the minimum moves to thicker active regions. $J_{\rm th}$ versus optical loss plots demonstrate that with the high optical losses in the materials grown, it will be easier to induce lasing in thick active region structures. Results for AlGaAs/GaAs lasers presented for comparison, demonstrate that AlGaN/GaN lasers have higher $J_{\rm th}$ unless the active region is very thin.**

I. Introduction

There is great interest in creating current injection pumped semiconductor lasers from the wide bandgap AlInGaN material system to obtain short wavelength light [1], [2]. Due to difficulties in growing high quality materials, this goal has only recently been achieved [3], [4]. Other devices based on the wide bandgap materials, such as light emitting diodes [5]–[7], transistors [8], and detectors [9], have been demonstrated. Numerical simulations of nitride based lasers are needed to give experimentalists some indication of the threshold currents expected with the materials available. There have been several theoretical predictions of gain and threshold currents in nitride based wide bandgap lasers [10]–[13]. However, these theoretical works have not taken into account the complete structure of the laser, and important factors such as charge carrier emission at heterojunctions, current spreading and carrier leakage out of the active region.

We have previously simulated InGaN/AlGaN light emitting diodes [14] and obtained results which agreed well with experiments, demonstrating that numerical simulations of wide bandgap nitride based semiconductor devices can aid in their development. We have now performed 2-D numerical simulations of semiconductor lasers using a version of the MINILASE [15] program which we have modified for wide bandgap laser simulations.

II. Simulation Procedure and Device Structure

The simulation program solves, over a 2-D cross section of the device, Poisson's equation, the electron and hole continuity equations, and the wave equation. Thermionic emission is included for electrons

Manuscript received February 23, 1996; revised August 8, 1996. The review of this brief was arranged by Editor P. K. Bhattacharya. This work was supported by the Army Research Office.

The authors are with the Department of Electrical and Computer Engineering, Wayne State University, Detroit, MI 48202 USA.

Publisher Item Identifier S 0018-9383(97)00325-0.

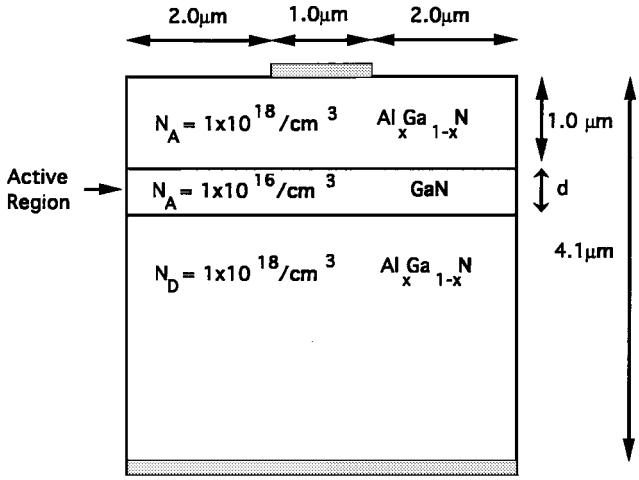

Fig. 1. Cross section of the AlGaN/GaN/AlGaN laser. d is the thickness of the active region.

and holes at the heterojunctions. The spontaneous recombination rate and gain are calculated by integrating the electron and hole distributions in the energy bands of the device according to formulas derived from Fermi's golden rule and assuming the k-selection rule holds [16]. The threshold for lasing is reached when the modal gain equals the optical losses present. Because improving material quality by reducing optical losses is an active research area, we have considered limiting cases of very low and very high optical losses to give an idea of the effects losses have on the threshold current density, $J_{\rm th}$, for different active region thicknesses and cavity lengths. All results are presented as injected current normalized only to the cavity length, $J_{\rm th}$, with units of [A/cm]. This is done because the lateral current spreading makes it impossible to define a uniform current per unit area in the device. For comparison all results can be divided by the top electrode's width, 1.0 μm, to get a value in [A/cm^2], though this value will be slightly larger than the actual $J_{\rm th}$ in the active region.

The double heterostructure (DH) edge emitting semiconductor laser's structure, dimensions and dopant concentrations are shown in Fig. 1. A narrow stripe laser is simulated here because this type of laser is able to produce enough saturable absorption for self sustained pulsations (SSP) to occur as was demonstrated for an AlGaAs laser in which SSP occurs for stripe widths less than 2.5 μm [17]. SSP is a practical method for reducing excess noise in semiconductor lasers, especially in the field of optical disc systems [18]. This is one field where there is great interest in blue to ultraviolet light emitters, because, with shorter wavelength light, the density of optically stored information is greater. The modal gain for the first order lasing mode, calculated considering the overlap of the optical field and the material's gain, will be larger in narrow stripe nitride based lasers than arsenide based lasers because the lower charge carrier mobility in the nitride based lasers leads to much less current spreading.

Parameter values for AlN and GaN are listed in Table I. Values for $\mathrm{Al}_x\mathrm{Ga}_{1-x}\mathrm{N}$ were obtained by taking corresponding proportions of the values for the constituent compounds. The band offset between AlN and GaN was taken as $\Delta E_c = 2.3$ eV [19], [20] and linearly scaled for $\mathrm{Al}_x\mathrm{Ga}_{1-x}\mathrm{N}/\mathrm{GaN}/\mathrm{Al}_x\mathrm{Ga}_{1-x}\mathrm{N}$ structures.

III. Results and Discussions

Fig. 2 demonstrates that $J_{\rm th}$ versus active region thickness, d, plots for $\mathrm{Al}_{0.4}\mathrm{Ga}_{0.6}\mathrm{N}/\mathrm{GaN}/\mathrm{Al}_{0.4}\mathrm{Ga}_{0.6}\mathrm{N}$ lasers, exhibit a minimum. Fig. 2(a) shows that the minimum of $J_{\rm th}$ occurs at $d = 0.1$ μm, for a 100-μm cavity laser in the ideal case of only mirror losses being present (loss $= 157$/cm), and as the losses increase the minimum shifts to larger d. Fig. 2(b) shows that the minimum $J_{\rm th}$ occurs at $d = 0.04$ μm, for a 500-μm laser with only mirror losses present (loss $= 32$/cm). These curves are limiting cases that are approached as optical losses due to scattering and absorption of light are reduced by improved material growth techniques. Though the longer cavity shows dramatic improvements in $J_{\rm th}$, the optical losses due to photon absorption and scattering will increase because the photons spend more time in the cavity; and the threshold may be much higher.

TABLE I
Material Parameters of A1N and GaN

parameter	AlN	GaN
m_e^*	0.48	0.2
m_h^*	0.7	0.4
μ_n $\left[\frac{\mathrm{cm}^2}{\mathrm{V\,s}}\right]$	300	600
μ_p $\left[\frac{\mathrm{cm}^2}{\mathrm{V\,s}}\right]$	14	9
$\epsilon_r(0)$	8.5	9.0
$\epsilon_r(\infty)$	4.7	5.35
ref. index	2.15	2.67
E_g [eV]	6.2	3.43
Δ_{SO} [meV]	0	11

The increase of $J_{\rm th}$ on the right of the minimum is due to the increased number of states population inversion should occur in, as d increases. The increase in $J_{\rm th}$ to the left of the minimum is due to the loss of confinement of light, to the active region, causing a reduction in the modal gain.

Curves for $\mathrm{Al}_{0.4}\mathrm{Ga}_{0.6}\mathrm{As}/\mathrm{GaAs}/\mathrm{Al}_{0.4}\mathrm{Ga}_{0.6}\mathrm{As}$ lasers with similar structure, and only mirror losses, are included in Fig. 2(a) (loss $=$ 115/cm) and Fig. 2(b) (loss $= 23$/cm) to show that AlGaN/GaN lasers have higher $J_{\rm th}$ unless the active region is very thin, eg. less than $d = 0.05$ μm for a 100-μm long cavity. Mirrors formed by cleaving give AlGaAs lasers an advantage of lower mirror losses, and in this limiting case, lower $J_{\rm th}$. Also, the curves for AlGaN/GaN lasers have a minimum located at smaller d because shorter wavelength light is more confined, increasing the modal gain in narrow waveguides; and larger curvature near the minimum.

The large increase of $J_{\rm th}$ on the left of the minimum for the AlGaN/GaN curves in Fig. 2(a), as the losses increase, demonstrates that for even higher optical loss materials, the threshold for lasing will be easier to reach if the active region is thicker than the thickness at the minimum $J_{\rm th}$. As an example, when $d = 0.2$ μm, $J_{\rm th}$ increases 1.1 A/cm when the losses increase from 157/cm to 320/cm. However, when the $d = 0.04$ μm, $J_{\rm th}$ increases by 16.5 A/cm for the same increase in losses.

Fig. 3 presents the mode confinement factors, which were obtained from a 2-D solution of the optical wave equation and used in these simulations, for the AlGaN/GaN and the AlGaAs/GaAs lasers. There is a smooth increase in the confinement factor for both lasers as the active region thickness increases, but the confinement factor is slightly larger for the nitride based laser, due in part to the propagation

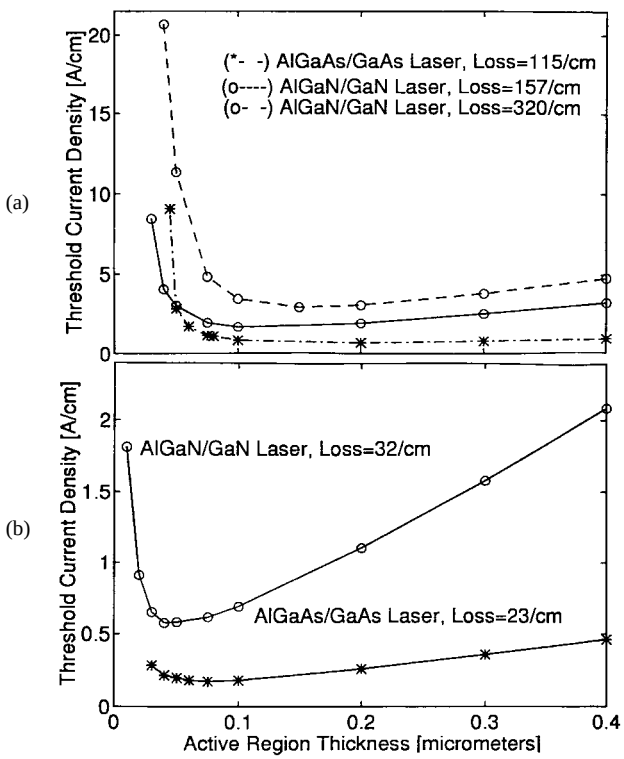

Fig. 2. Dependence of the threshold current on active region thickness for $Al_{0.4}Ga_{0.6}N/GaN/Al_{0.4}Ga_{0.6}N$ and $Al_{0.4}Ga_{0.6}As/GaAs/Al_{0.4}Ga_{0.6}As$ lasers. (a) Loss values of 115/cm and 157/cm represent the limiting case of a laser with only mirror losses and a cavity length of 100 μm. (b) Loss values are for the limiting case of a laser with a 500-μm long cavity containing only mirror losses.

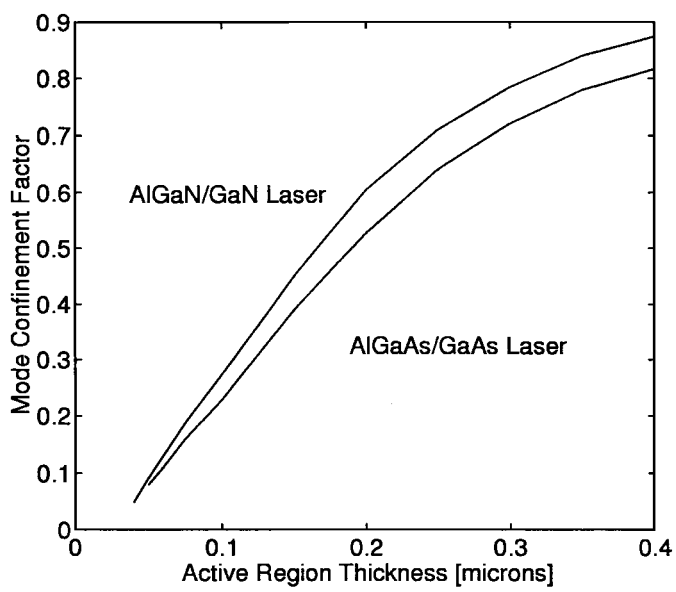

Fig. 3. Mode confinement factors for the $Al_{0.4}Ga_{0.6}N/GaN/Al_{0.4}Ga_{0.6}N$ and $Al_{0.4}Ga_{0.6}As/GaAs/Al_{0.4}Ga_{0.6}As$ lasers.

of shorter wavelength light. As the active region's thickness is reduced, the confinement factors approach one another indicating that mode confinement has a minor role in the difference in behavior at very narrow active region thicknesses.

Maximum gain versus nominal current density is plotted in Fig. 4 for a GaN laser. Nominal current density equals the current lost to

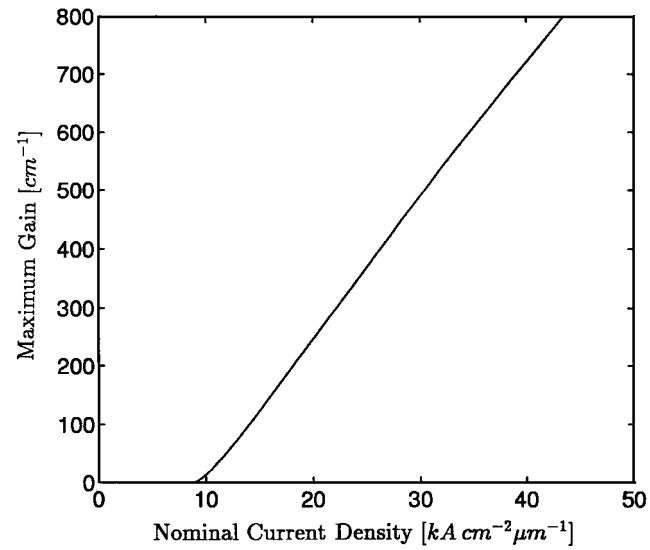

Fig. 4. Maximum gain versus nominal current density for a GaN active region laser.

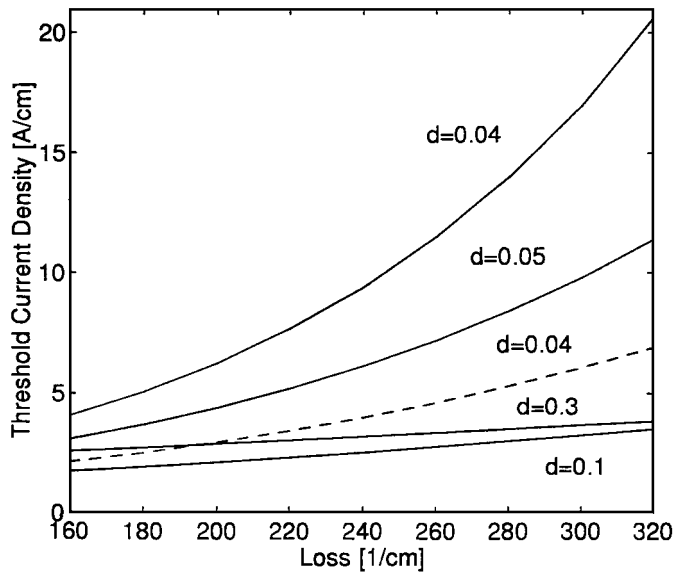

Fig. 5. Threshold current as a function of the total optical losses for $Al_{0.4}Ga_{0.6}N/GaN/Al_{0.4}Ga_{0.6}N$ lasers with $d = 0.04$ μm, 0.05 μm, 0.1 μm, and 0.3 μm. The dashed line (- - -) shows the behavior of the threshold current for $Al_{0.8}Ga_{0.2}N/GaN/Al_{0.8}Ga_{0.2}N$ lasers with $d = 0.04$ μm.

radiative recombination in a double heterostructure laser [16]. For the AlGaN/GaN laser with a loss of 320/cm, Fig. 2(a) shows that the minimum threshold current is 3 A/cm and occurs in a DH structure with an active region thickness of 0.15 μm. Fig. 4 demonstrates that if all the injected carriers recombined radiatively, the equivalent threshold current would be between 0.343 A/cm and 1.72 A/cm. These values are obtained by multiplying the nominal current density required for a gain of 320/cm by the active region thickness and either the stripe's width or the active region's width, respectively. Because of current spreading, the true value that should be used here is between these two extreme values. The increased threshold current obtained in the simulations demonstrates that complete 2-D numerical simulations are necessary to account for the loss of carriers through mechanisms other than radiative recombination as well as the effect of the true mode confinement factor on modal gain.

Fig. 5 demonstrates that for thinner active regions than at the minimum in the low loss curve for the AlGaN/GaN laser in Fig. 2(a), (e.g., $d = 0.04$ μm or $d = 0.05$ μm.) there is a fast increase in $J_{\rm th}$ as the losses increase. On the other hand, for thicker active regions than at the minimum, (e.g., $d = 0.3$ μm.) there is a slow rate of increase in $J_{\rm th}$ as the losses increase. This figure also shows $J_{\rm th}$'s rate of increase is higher when higher optical losses are present.

These effects occur because of the following scenario observed in these simulations. As the losses increase, the current density required at threshold increases. However, as d decreases the number of carriers that traverse the active region without recombining increases. Because of the large barrier, thermionic emission of charge carriers out of the active region is low. These carriers accumulate in the active region causing the quasi-Fermi levels to move further into the bands. Charge carriers with energies near the quasi-Fermi levels, therefore, have a lower barrier to surmount and can easily leave without recombining or increasing the gain.

With increased charge carrier confinement to the active region, by larger barriers, the threshold current is lower and has a smaller rate of increase as the losses increase. This is demonstrated by the dashed curve in Fig. 5, which is for an $Al_{0.8}Ga_{0.2}N/GaN/Al_{0.8}Ga_{0.2}N$ laser. This laser has a barrier of 1.84 eV for electrons in the active region compared to a barrier of 0.92 eV for the other curves in Fig. 5.

IV. Conclusion

In summary, we have investigated threshold current density versus active region thickness for AlGaN/GaN lasers for different optical loss values and compared these to curves for AlGaAs/GaAs lasers. Our results indicate that greater success in developing wide bandgap lasers will occur with DH lasers having active regions thicker than at the minimum in the $J_{\rm th}$ versus d curve. Other methods for increasing confinement of carriers such as using stopper layers will cause further reduction in the lasing threshold current densities of very narrow active region lasers [14], [21].

Acknowledgment

The authors would like to acknowledge K. Hess of the University of Illinois for providing an earlier version of the MINILASE [15] program and collaboration on our first paper.

References

[1] M. A. Khan, S. Krishnankutty, R. A. Skogman, J. N. Kuznia, D. T. Olson, and T. George, "Vertical-cavity stimulated-emission from photopumped InGaN/GaN heterojunctions at room temperature," *Appl. Phys. Lett.*, vol. 65, p. 520, 1994.

[2] X. H. Yang, T. J. Schmidt, W. Shan, J. J. Song, and B. Goldenberg, "Above room-temperature near-ultraviolet lasing from an optically pumped GaN film grown on sapphire," *Appl. Phys. Lett.*, vol. 66, p. 1, 1995.

[3] S. Nakamura, M. Senoh, S. Nagahama, N. Iwasa, T. Yamada, T. Matsushita, H. Kiyoku, and Y. Sugimoto, "InGaN-Based multi-quantum-well structure laser diodes," *Jpn. J. Appl. Phys.*, vol 35, 1996.

[4] ——, "InGaN multi-quantum-well laser diodes grown on $MgAl_2O_4$ substrates," *Appl. Phys. Lett.*, vol. 68, p. 2105, 1996.

[5] B. Goldenberg, J. D. Zook, and R. J. Ulmer, "Ultraviolet and violet light-emitting GaN diodes grown by low-pressure metalorganic chemical vapor-deposition," *Appl. Phys. Lett.*, vol. 62, p. 381, 1993.

[6] I. Akasaki, H. Amano, H. Murakami, M. Sassa, H. Kato, and K. Manabe, "Growth of GaN and AlGaN for UV blue p-n-junction diodes," *J. Cryst. Growth*, vol. 128, p. 379, 1993.

[7] R. J. Molnar, R. Singh, and T. D. Moustakas, "Blue-Violet light emitting gallium nitride p-n-junctions grown by electron-cyclotron resonance-assisted molecular-beam epitaxy," *Appl. Phys. Lett.*, vol. 66, p. 268, 1995.

[8] M. A. Khan, J. N. Kuznia, D. T. Olson, W. J. Schaff, J. W. Burm, and M. S. Shur, "Microwave performance of a 0.25-micrometer gate AlGaN/GaN heterostructure field-effect transistor," *Appl. Phys. Lett.*, vol. 65, p. 1121, 1994.

[9] M. A. Khan, J. N. Kuznia, D. T. Olson, M. Blasingame, and A. R. Bhattarai, "Schottky-Barrier photodetector based on Mg-doped p-type GaN films," *Appl. Phys. Lett.*, vol. 63, p. 2455, 1993.

[10] W. W. Chow, A. Knorr, and S. W. Koch, "Theory of laser gain in group III nitrides," *Appl. Phys. Lett.*, vol 67, p. 754, 1995.

[11] P. Rees, C. Cooper, P. M. Smowton, P. Blood, and J. Hegarty, "Calculated threshold currents of nitride and phosphide based quantum well lasers," *IEEE Photon. Technol. Lett.*, vol. 8, p. 197, 1996.

[12] W. Fang and S. L. Chaung, "Theoretical prediction of GaN lasing and temperature sensitivity," *Appl. Phys. Lett.*, vol. 67, p. 751, 1995.

[13] A. T. Meney, E. P. O'Reilly and A. R. Adams, "Optical gain in wide bandgap GaN quantum well lasers," *Semicond. Sci. Technol.*, vol 11, p. 897, 1996.

[14] P. Shah, V. Mitin, K. Hess, M. Grupen, and G. H. Song, "Numerical simulation of wide bandgap AlGaN/InGaN light emitting diodes for output power characteristics and emission spectra," *J. Appl. Phys.*, vol. 79, p. 2755, 1996.

[15] G. H. Song, "Two-dimensional simulation of quantum-well lasers including energy transport (semiconductor lasers)," Ph.D. dissertation, Univ. of Illinois, Urbana-Champaign, 1990.

[16] G. P. Agrawal and N. K. Dutta, *Semiconductor Lasers*. New York: Van Nostrand Rheinhold, 1993.

[17] M. Yuri, J. S. Harris, Jr., T. Takayama, O. Imafuji, H. Naito, M. Kume, K. Itoh, and T. Baba, "Two-dimensional analysis of self-sustained pulsation for narrow-stripe AlGaAs lasers," *IEEE J. Select. Topics Quantum Electron.*, vol. 1, p. 473, 1995.

[18] M. Yamada, "A theoretical analysis of self-sustained pulsation phenomena in narrow stripe semiconductor lasers," *IEEE J. Quantum Electron.*, vol. 29, p. 1330, 1993.

[19] J. Baur, K. Maier, M. Kunzer, U. Kaufmann, and J. Schneider, "Determination of the GaN/AlN band-offset via the (-/0)- acceptor level of iron," *Appl. Phys. Lett.*, vol. 65, p. 2211, 1994.

[20] G. Martin, S. Strite, A. Botchkarev, A. Agarwal, A. Rockett, W. R. L. Lambrecht, B. Segall, and H. Morkoc, "Valence-band discontinuity between GaN and AlN measured by X-ray photoemission spectroscopy," *J. Electron. Mater.*, vol. 24, p. 225, 1995.

[21] S. Nakamura, T. Mukai, and M. Senoh, "Candela-class high brightness InGaN/AlGaN double heterostructure blue-light emitting diodes," *Appl. Phys. Lett.*, vol. 64, p. 1687, 1994.